FUDMA Journal of Sciences (FJS)
ISSN online: 2616-1370
ISSN print: 2645 - 2944
Vol. 10 No. 23, December (Special Issue), 2026, pp 29 – 37
DOI: https://doi.org/10.33003/fjs-2026-1023-6574

Regularised Geoadditive Regression Modelling of Malaria Cases in the North-Western Region of Nigeria

[*]Razinu Hamisu Ayuba and Saheed Olalenkan Jabaru

Department of Physical Sciences, Faculty of Natural and Applied Sciences, Al-Hikmah University, Ilorin, Nigeria

*Corresponding authors' email: razinuhamisuayuba@gmail.com

Received: 25 Sept. 2026
Accepted: 22 Nov. 2026
Published: 27 Nov. 2026

ABSTRACT
Malaria remains a major public health problem in Nigeria, particularly in the North-West. Environmental, spatial and temporal factors shape its distribution but are rarely modelled together, and conventional regression assumes linear effects and independent observations, risking biased estimates and missed hotspots. The aim of this study was to assess environmental and spatial risk factors of malaria in North-Western Nigeria using a Regularised Geoadditive Regression Model (RGRM). Secondary state-level data for 2015–2024 (70 state-year observations) came from DHIS2, remote-sensing platforms, WorldPop and national surveys. Confirmed cases were overdispersed, so Negative Binomial models fitted by restricted maximum likelihood progressed from a Generalised Additive Model to a Geoadditive Model then the RGRM, combining penalised splines, spatial and temporal terms, and shrinkage penalties. Global, yearly and local (LISA) Moran's I statistics tested spatial autocorrelation, and state-level random intercepts identified residual spatial effects. Distance to water was the only significant linear predictor (incidence rate ratio = 0.9917, $p < 0.001$), and elevation was significant among the smooth terms ($p = 0.005$). The spatial surface and temporal trend were significant ($p < 0.001$), with expected cases rising about five-fold between 2015 and 2024. Cases were significantly clustered (Moran's I = 0.1850, $p = 0.033$), with Kano, Katsina and Kaduna forming a high-burden core, whereas residuals showed no significant clustering ($p = 0.657$) or state-level effects. Malaria burden is spatially clustered, rising over time and strongly associated with proximity to water. Control programmes should therefore prioritise communities near water and coordinate surveillance across state borders.

Keywords: Malaria, Geoadditive Regression, Spatial Autocorrelation, Negative Binomial Model, North-Western Nigeria

INTRODUCTION

Malaria caused an estimated 263 million cases and 597,000 deaths globally in 2023, with Nigeria contributing about 26% of cases and 31% of deaths (World Health Organization [WHO], 2024). Transmission depends on climate, vegetation, elevation and proximity to water (Githeko *et al.*, 2000; Patz *et al*., 2005). The North-West remains a high-burden zone, with marked variation between its seven states (Eshofonie *et al.*, 2025; Isiko *et al.*, 2024; Ogunsakin *et al.*, 2024).

Previous Nigerian studies identified community risk factors in Kano (Dawaki *et al.*, 2016), spatial clustering in Jigawa (Yakudima *et al.*, 2024), and potential benefits of treatment and net coverage through compartmental models in Kano and Kebbi (Bakare *et al.*, 2026; Dambazau *et al.*, 2025). Ugwu and Zewotir (2020) found nonlinear environmental effects using generalised additive models. Other studies examined environmental associations, hotspots, child risk and net ownership (Bayode & Siegmund, 2024; Ekpa *et al.*, 2023; Isiko *et al.*, 2024; Ogidan *et al.*, 2025; Ogunsakin *et al.*, 2024). Eshofonie *et al.* (2025) used joint Bayesian modelling. Studies elsewhere examined malaria control, nonlinear temperature responses, risk mapping and additive models (Bhatt *et al.*, 2015; Bosson-Amedenu *et al.*, 2026; Mordecai *et al.*, 2013; Zhang *et al.*, 2024).

Ogbuagada *et al.* (2022) modelled monthly malaria cases in Jimeta, Adamawa State, using vector autoregression, providing further evidence of the use of time-series methods for malaria modelling in Nigeria.

These studies leave a need for joint analysis of nonlinear environmental effects, spatial dependence and temporal trends in routinely reported case counts across all seven North-Western states. Environmental responses can be nonlinear (Mordecai *et al.*, 2013; Yamana & Eltahir, 2013), while neighbouring areas share conditions and movement patterns (Tobler, 1970). Spatial methods are important for malaria mapping (Odhiambo *et al.*, 2020). Geoadditive models combine nonlinear effects with a spatial surface (Cressie, 1993; Kammann & Wand, 2003); regularisation limits complexity by shrinking weak terms (Tibshirani, 1996; Zou & Hastie, 2005).

The aim of this study was to apply a Negative Binomial Regularised Geoadditive Regression Model (RGRM) to annual confirmed malaria cases in North-Western Nigeria, 2015–2024, to assess environmental risk factors, test spatial autocorrelation, and examine residual state effects after adjustment. We hypothesised that malaria cases in North-Western Nigeria change nonlinearly with environmental factors and depend on space and time, and that the RGRM would fit the data better than a standard GAM.

MATERIALS AND METHODS

Study Area and Design

The study covered Jigawa, Kaduna, Kano, Katsina, Kebbi, Sokoto and Zamfara States. The area has distinct wet and dry seasons, Sudan and Sahel savannah vegetation, and substantial environmental variation.

The design was quantitative, non-experimental and ecological, using secondary state-level data for 2015-2024. The state-year was the unit of analysis, giving $7 \times 10 = 70$

observations. All available records were analysed, so no sampling was involved.

Study Variables

The response variable was the annual number of confirmed malaria cases per state (cases per year), diagnosed by microscopy or rapid diagnostic test and reported through the District Health Information System 2 (DHIS2), the national health information platform managed by the NMEP under the Federal Ministry of Health. Explanatory variables, with their units, were average annual temperature (°C), total annual rainfall (mm), mean relative humidity (%), the normalised difference vegetation index (NDVI, an index from −1 to +1), the normalised difference built-up index (NDBI, an index from −1 to +1), distance to water (km), elevation (m above sea level), cropland cover (% of land area), population density (persons per km²), poverty rate (%), and insecticide-treated net (ITN) use (% of people sleeping under a net) among under-five children, pregnant women and the whole population. Longitude and latitude of the state centroids represented location. Rainfall and temperature were extracted from TerraClimate (Abatzoglou *et al.*, 2018) and relative humidity from ERA5-Land (Muñoz-Sabater *et al.*, 2021) through Google Earth Engine (Gorelick *et al.*, 2017). NDVI came from MODIS (Didan, 2021), NDBI from Landsat 8 imagery (Roy *et al.*, 2014), cropland cover from the ESA WorldCover dataset (Zanaga *et al.*, 2021), elevation from the Shuttle Radar Topography Mission (Farr *et al.*, 2007), distance to water from surface-water layers, and population density from WorldPop (n.d.). Poverty and ITN indicators came from the Nigeria Malaria Indicator Survey (National Malaria Elimination Programme *et al.*, 2022), the Nigeria Demographic and Health Survey (Federal Ministry of Health and Social Welfare *et al.*, 2025) and the National Bureau of Statistics, and state boundaries from the GADM database (GADM, 2022) were used for spatial analysis.

Statistical Models

Confirmed case counts were modelled using a Negative Binomial distribution with mean μ_{it} and dispersion θ to allow overdispersion. A log link connected the mean to the predictor, as shown in Equation (1):

$$Y_{it} \sim NB(\mu_{it}, \theta), Var(Y_{it}) = \frac{\mu_{it} + \mu_{it}^2}{\theta} \quad (1)$$

where θ is the dispersion parameter, and a log link connects μ_{it} to the linear predictor. Three models were fitted in sequence to the same 70 observations (Hastie & Tibshirani, 1990; McCullagh & Nelder, 1989; Nelder & Wedderburn, 1972).

Generalised Additive Model (GAM). Poverty rate, the three ITN indicators (under-fives, pregnant women and general population), NDBI and distance to water were treated as linear covariates, while temperature, rainfall, relative humidity, NDVI, elevation, population density and cropland were represented by penalised smooth functions.

$$\log(\mu_{it}) = \beta_0 + \sum_{k=1}^{6} \beta_k x_k + \sum_{j=1}^{7} f_j(Z_{jit}) \quad (2)$$

where x_k are the linear covariates and Z_j the seven smoothed covariates. Each f_j was a penalised spline, with smoothness selected by REML to balance fit and complexity.

Geoadditive Regression Model (GRM). A spatial surface, estimated as a two-dimensional thin-plate (kriging-type) spline over longitude and latitude, was added to the GAM to account for residual spatial structure.

$$\log(\mu_{it}) = \beta_0 + \sum_{k=1}^{6} \beta_k x_k + \sum_{j=1}^{7} f_j(Z_{jit}) + S(lon_i, lat_i) \quad (3)$$

Regularised Geoadditive Regression Model (RGRM). The final model added a smooth temporal trend $f_{time}(year_t)$ and a state-level random intercept ui. Regularisation penalised weak model components to reduce overfitting and improve stability with the small sample size.

$$\log(\mu_{it}) = \beta_0 + \sum_{k=1}^{6} \beta_k x_k + \sum_{j=1}^{7} f_j(Z_{jit}) + S(lon_i, lat_i) + f_{time}(year_t) + u_i, \quad (4)$$

Linear effects were reported as incidence rate ratios (IRR = exp(β)), representing multiplicative changes in expected cases. Smooth effects were assessed using approximate Wald tests.

Estimation of The Smoothing Parameters

The smooth functions were estimated using penalised B-splines (P-splines). The degree of smoothness was controlled by smoothing parameters (λ), which were estimated using Restricted Maximum Likelihood (REML). The penalised log-likelihood is expressed as:

$$PL(\beta) = L(\beta) - \sum_{j=1}^{7} \lambda_j J(f_j) \quad (5)$$

Where, $L(\beta)$ is the log-likelihood function; $J(f_j)$ is the roughness penalty for the j-th smooth function; λ_j is the smoothing parameter controlling the balance between model fit and smoothness.

The smooth functions are P-splines (Eilers & Marx, 1996). The REML method (Wood, 2011) estimates the smoothing parameters automatically, thereby reducing overfitting and improving the stability and predictive performance of the model.

Model Significance Testing

Approximate Chi-square (Wald-type) for testing the significance of the nonlinear smooth terms:

$$\chi_j^2 = f_j^T V_j^{-1} f_j \quad (6)$$

Then approximately,

$$\chi_j^2 \sim \chi_j^2(EDF_j)$$

where, $\hat{f}_j$ is the vector of estimated values of the j-th smooth function; V_j is the estimated covariance matrix; EDF_j is the effective degrees of freedom for the smooth term.

Spatial Autocorrelation

Moran's I test was used to detect spatial autocorrelation in malaria cases and in model residuals:

$$I = \frac{n}{W} \times \frac{\sum_i \sum_j w_{ij}(x_i - \bar{x})(x_j - \bar{x})}{\sum_i (x_i - \bar{x})^2} \quad (7)$$

Where n is the number of states, x_i and x_j are the values (malaria cases or model residuals) for states i and j, $\bar{x}$ is their mean, w_{ij} are the spatial weights and $W = \sum_i \sum_j w_{ij}$

A k-nearest-neighbour matrix (k = 3) was used. Applied to the model residuals, the test determines whether malaria cases remain spatially clustered after adjusting for the explanatory variables. Global Moran's *I* was calculated for the ten-year mean and separately for each year; local Moran's *I* (LISA) identified significant local clusters at the 5% level.

Residual State Effects

The combined geographic contribution was S (lon, lat) + ui. State random-intercept significance was assessed using its standard error, with relative risk RR = exp(ui). The reported random-intercept intervals do not quantify uncertainty in the combined geographic contribution.

All analyses were done in R (R Core Team, 2024), using the additive modelling methods described by Wood (2017).

RESULTS AND DISCUSSION

Model Building

Each modelling step improved fit (Table 1). Adding the spatial surface to the GAM lowered AIC from 1,958.9 to 1,953.4, while the RGRM further reduced it to 1,923.3.

Deviance explained increased from 88.3% in the GAM to 90.4% in the GRM and 92.0% in the RGRM.

Table 1: Comparison of The Fitted Negative Binomial Models (N = 70)

Model	AIC (lower is better)	Deviance explained (%)	Adjusted R^2 (0 to 1)	θ (dispersion)
GAM	1,958.9	88.33	0.8057	14.31
GRM (GAM + spatial surface)	1,953.4	90.37	0.8255	16.28
RGRM (GRM + trend, random intercept, shrinkage)	1,923.3	92.03	0.8885	22.44

AIC = Akaike information criterion; θ = Negative Binomial dispersion parameter.

The earlier models gave a different picture of the covariates. In the GAM, population density was the strongest apparent predictor, but its effect weakened after spatial and temporal structures were added. This indicates that part of the apparent population effect was associated with location and time rather than an independent environmental relationship.

Environmental Risk Factors

The final fitted equation was $\log(\mu) = 15.0267 - 0.0001\ \text{Poverty} - 0.0013\ \text{ITN}_{U5} + 0.0008\ \text{ITN}_{PW} + 0.0016\ \text{ITN}_{Pop} - 6.4024\ \text{NDBI} - 0.0083\ \text{DistWater} + \text{smooth terms} + S(\text{lon, lat}) + f_{\text{time}}(\text{year}) + u_i$, with $\theta = 22.44$. Table 2 gives the linear effects and Table 3 the smooth, spatial and temporal terms.

Table 2: Linear Effects in The Final Rgrm

Term	Estimate (log scale)	IRR (ratio)	SE (log scale)	p-value
Intercept	15.0267	3,357,448.56	0.2798	<0.0001
Poverty rate	−0.0001	0.9999	0.0034	0.9752
ITN use, under-fives	−0.0013	0.9987	0.0093	0.8896
ITN use, pregnant women	0.0008	1.0008	0.0064	0.8992
ITN use, general population	0.0016	1.0016	0.0109	0.8852
NDBI	−6.4024	0.0017	3.3256	0.0542
Distance to water (per km)	**−0.0083**	**0.9917**	**0.0017**	**<0.0001**

IRR = incidence rate ratio, exp(estimate); SE = standard error. The intercept refers to a hypothetical state with all covariates equal to zero and is not interpreted.

Only one linear predictor was clearly significant. Distance to water had a negative coefficient (IRR = 0.9917, $p < 0.001$), indicating that expected malaria cases decreased by about 0.83% per additional kilometre from water (about 8% for every additional 10 km), holding other terms constant. Poverty, ITN use, NDBI and the other linear terms were not significant.

Table 3: Smooth, Spatial, Temporal and Random Terms in The Final RGRM

Term	Component	Edf	χ^2	p-value
s(Temp)	Temperature	0.000	0.00	0.9909
s(Rain)	Rainfall	0.000	0.00	0.6425
s(Hum)	Relative humidity	1.097	2.92	0.0559
s(NDVI)	Vegetation index	0.000	0.00	0.6738
s(Elev)	Elevation	0.709	2.43	0.0052*
s(PopDen)	Population density	0.000	0.00	0.9892
s(Crop)	Cropland cover	0.000	0.00	0.3562
s(lon, lat)	Spatial surface	3.354	42.94	<0.0001*
s(year)	Temporal trend	1.967	264.23	<0.0001*
s(state)	State random intercept	0.001	0.00	0.2977

*edf = effective degrees of freedom; χ^2 = Wald statistic; * significant at the 5% level.*

Regularisation reduced the contribution of several environmental smooths. Temperature, rainfall, NDVI, population density and cropland were shrunk effectively to zero, while humidity remained weak and nonsignificant. Elevation retained a significant effect ($p = 0.005$); its curve rises gently (Figure 1), so higher-lying states had somewhat more cases after adjustment for space and time, although the confidence band is wide.

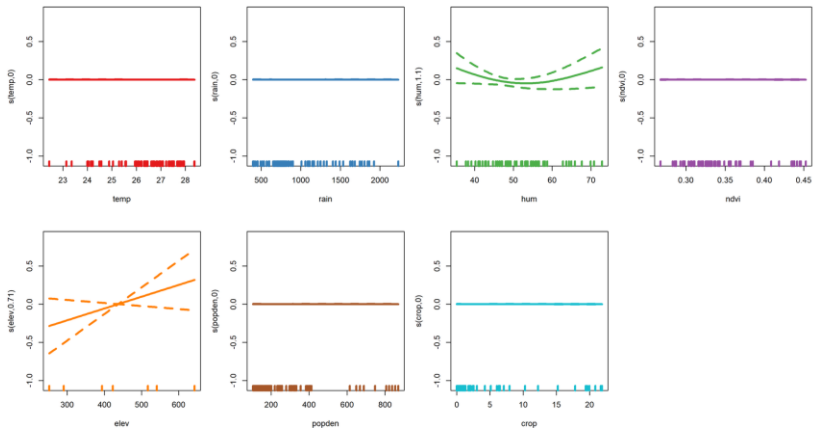

Figure 1: Smooth Effects of the Environmental Covariates in The Final RGRM. Solid Lines Are the Estimated Smooth Functions and Dashed Lines Are 95% Confidence Bands; Terms Shrunk to Zero Appear as Flat Lines. Rug Marks Show Where the Observations Lie

The spatial surface (edf = 3.35, χ^2 = 42.94, p < 0.001) and temporal trend (edf = 1.97, χ^2 = 264.23, p < 0.001) were highly significant. The temporal curve showed a steady rise in expected cases, with 2024 approximately five times the 2015 level after adjustment. The random-intercept distribution was centred near zero, with no evidence of major unexplained state-level variation.

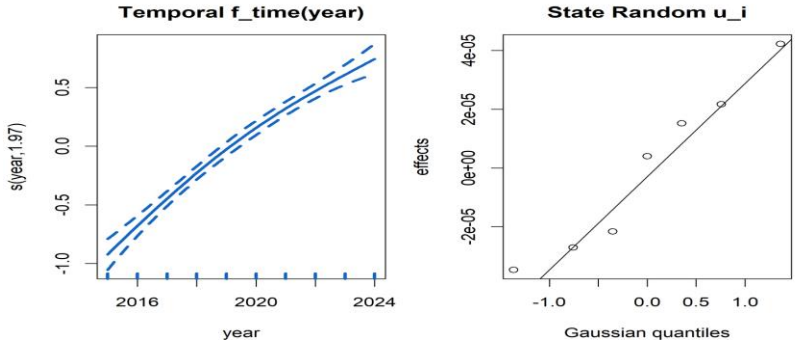

Figure 2: Estimated Temporal Trend, F_{time}(Year) (Left), And Normal Q–Q Plot of the State Random Intercepts, U_i (Right), From The Final RGRM

Spatial Autocorrelation

Malaria cases were significantly clustered. Global Moran's I for the ten-year mean was 0.1850 (p = 0.033), indicating positive spatial autocorrelation. The corresponding Moran's I for RGRM residuals was not significant (p = 0.657), suggesting that the model accounted for the main spatial dependence.

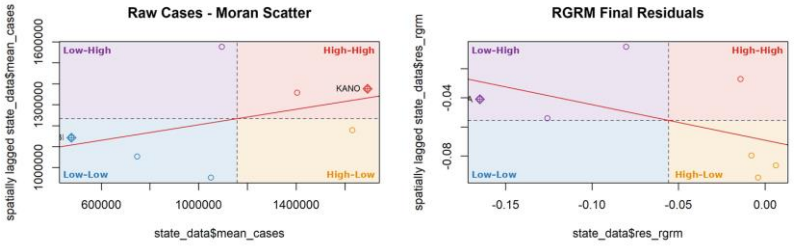

Figure 3: Moran's I Scatter Plot for The Ten-Year Mean of Malaria Cases (Left) And for The Residuals of the Final RGRM (Right)

Clustering varied across years (table 4) and was significant in six of the ten years: 2015, 2018, 2019, 2020, 2021 and 2024.

Table 4: Yearly Global Moran's I for Malaria Cases, 2015–2024

Year	Moran's I	E(I)	p-value	Pattern
2015	0.1705	−0.1667	0.0147*	Clustered
2016	0.0399	−0.1667	0.1118	Random
2017	−0.0367	−0.1667	0.2328	Random
2018	0.1637	−0.1667	0.0363*	Clustered
2019	0.2087	−0.1667	0.0302*	Clustered
2020	0.1879	−0.1667	0.0409*	Clustered
2021	0.2703	−0.1667	0.0153*	Clustered
2022	−0.0303	−0.1667	0.2122	Random
2023	−0.1376	−0.1667	0.4341	Random
2024	0.2324	−0.1667	0.0213*	Clustered

** significant at the 5% level.*

The local analysis was more limited (Table 5, Figure 4). Jigawa was the only state identified as a significant local outlier, forming a Low–High pattern ($p < 0.05$).

Table 5: Local Moran's I (LISA) for Mean Malaria Cases

State	Mean cases (cases per year)	Local I (no unit)	Z-score (no unit)	p-value	Cluster type
Jigawa	1,094,763	−0.1499	−2.033	0.0421*	Low–High
Kaduna	1,404,253	0.2846	1.235	0.2169	Not significant
Kano	1,693,000	0.6771	1.802	0.0715	Not significant
Katsina	1,630,640	0.0585	0.563	0.5736	Not significant
Kebbi	477,737	0.0546	0.846	0.3978	Not significant
Sokoto	1,050,745	0.1252	1.112	0.2663	Not significant
Zamfara	747,509	0.2447	0.933	0.3508	Not significant

** significant at the 5% level.*

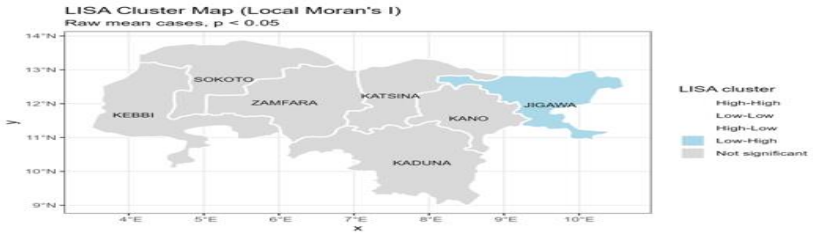

Figure 4: LISA cluster map of mean malaria cases ($p < 0.05$). Jigawa is the only significant cluster (Low–High)

Geographic Contributions and State Random Effects

No state random intercept was significant (Table 6); their relative risks were approximately 1. The spatial surface nevertheless varied between states. Table 6 and Figure 5 show the combined geographic contribution separately from the random-intercept uncertainty.

Table 6: State Random-Intercept Estimates and Fitted Geographic Contributions in The Final RGRM

State	u_i	RR (95% CI)	p-value	S(lon, lat)	S + u_i
Katsina	0.000	1.000 (0.997–1.003)	0.9947	0.3487	0.3487
Kano	0.000	1.000 (0.997–1.003)	0.9957	0.2225	0.2225
Sokoto	0.000	1.000 (0.997–1.003)	0.9962	0.1956	0.1956
Jigawa	0.000	1.000 (0.997–1.003)	0.9988	0.0077	0.0077
Kaduna	0.000	1.000 (0.997–1.003)	0.9984	−0.0209	−0.0209

State	u_i	RR (95% CI)	p-value	S(lon, lat)	S + u_i
Zamfara	0.000	1.000 (0.997–1.003)	0.9966	−0.0541	−0.0541
Kebbi	0.000	1.000 (0.997–1.003)	0.9958	−0.6995	−0.6995

u_i = state random intercept (SE = 0.0015 for every state); RR = exp(u_i); S(lon, lat) = spatial surface; S + u_i = total residual spatial effect.

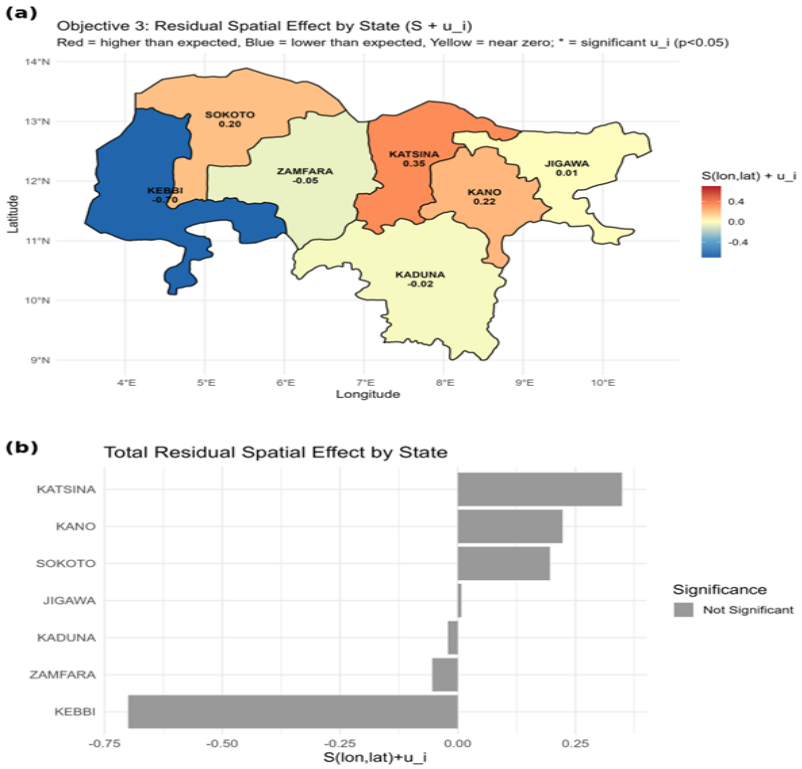

Figure 5: Fitted Geographic Contribution by State, S (Lon, Lat) + Ui: (A) Map and (B) Ranked Bar Chart. Table 6 Tests The Random Intercepts; Uncertainty in The Combined Contribution Was Not Reported

Discussion

Environmental Determinants

Distance to water was the only significant linear predictor: expected cases declined by about 0.83% per additional kilometre. This agrees with the proximity-to-water association reported by Ugwu and Zewotir (2020). Standing-water habitats can support mosquito breeding (Githeko *et al.*, 2000). The ecological association does not establish individual-level causation.

Elevation retained a significant positive smooth effect (p = 0.005), with considerable uncertainty. Ugwu and Zewotir (2020) found higher prevalence below approximately 500 m. Differences may reflect the present study's narrow range of state-average elevations, aggregation and adjustment for spatial and temporal terms.

Temperature, rainfall and humidity were not significant after adjustment, unlike environmental associations reported by Eshofonie *et al.* (2025), Ogunsakin *et al.* (2024), Ugwu and Zewotir (2020), and Mordecai *et al.* (2013). The findings partly agree with Ekpa *et al.* (2023). Annual state averages, a small sample, shared spatial and temporal signals, and shrinkage may explain weaker effects. Nonsignificance does not establish that climate is unimportant.

ITN use and poverty were not significant, unlike associations reported by Dawaki *et al.* (2016), Bayode and Siegmund (2024), Ogunsakin *et al.* (2024), and the continental benefits of nets reported by Bhatt *et al.* (2015). Isiko *et al.* (2024) reported a different direction of association for treated-net households. State averages may mask household variation, while programmes may distribute nets where burden is high. Ogidan *et al.* (2025) reported comparatively high ownership in the North-West. Population density was shrunk to zero. The negative NDBI coefficient was nonsignificant (p = 0.054), although its direction is consistent with urbanisation-related reductions described by Tatem *et al.* (2013).

Temporal Trend and Rising Malaria Burden

The adjusted temporal trend implied roughly five times as many expected cases in 2024 as in 2015. This contrasts with the earlier continental decline (Bhatt *et al.*, 2015), but overlaps a period of increased Nigerian survey prevalence described by Ogunsakin *et al.* (2024). Counts and prevalence are different outcomes: population growth, testing and reporting changes may contribute to the observed trend. Its cause cannot be established by this model.

Spatial Clustering and Residual Effects

Mean cases were spatially clustered (Moran's I = 0.1850), as in studies of Jigawa and Nigeria (Eshofonie *et al.*, 2025; Ogunsakin *et al.*, 2024; Ugwu & Zewotir, 2020; Yakudima *et al.*, 2024). The smaller coefficient may reflect aggregation into seven large units. High Kano counts are consistent with the burden considered by Dambazau *et al.* (2025). Jigawa's Low–High pattern here can coexist with within-state hotspots

reported by Yakudima *et al.* (2024). Kebbi's low reported counts differ from its high prevalence in Eshofonie *et al.* (2025), warranting checks of reporting and population denominators.

Residual autocorrelation was nonsignificant (p = 0.657), suggesting that the model captured much of the geographic dependence. State random intercepts were also nonsignificant. These findings extend descriptive hotspot analyses (Bayode & Siegmund, 2024; Ogunsakin *et al.*, 2024; Yakudima *et al.*, 2024), but do not prove that states have identical risk. The uncertainty intervals in Table 6 apply to random intercepts, not to the combined spatial surface and random effect.

Strengths and Limitations

Strengths include staged model comparison, regularisation with 70 observations, combined environmental and intervention indicators, and checks of raw and residual spatial dependence. The 92.03% deviance explained is an in-sample fit measure; it is not directly comparable with the 44.2% OLS variation explained in Ogunsakin *et al.* (2024). Limitations include ecological aggregation, reporting differences, annual resolution, only seven spatial units, and difficulty separating state-constant elevation and distance to water from the spatial surface. No causal individual-level interpretation is supported. Future studies should use reliable LGA-level and monthly data and assess out-of-sample performance.

CONCLUSION

Malaria in North-Western Nigeria is a growing and geographically structured problem. The RGRM showed that spatial and temporal structure were more important than most individual environmental covariates. Distance to water and elevation were the main detectable environmental correlates, while the fitted spatial surface captured significant geographic variation. The model also removed residual spatial autocorrelation, supporting its usefulness for this state-level dataset.

i. Focus vector control near water: State programmes and the NMEP should give priority to settlements near rivers, dams, irrigation schemes and seasonal ponds when planning larval source management, indoor residual spraying and net distribution.
ii. Coordinate across state lines: Kano, Katsina, Kaduna and Jigawa in particular should time and align campaigns and share surveillance data, rather than treating state borders as the edge of the problem.
iii. Investigate reporting and access: Katsina and Kano programmes should examine health-facility access, treatment-seeking and cross-border movement; Kebbi should assess whether low reported counts reflect transmission or incomplete reporting.
iv. Sustain net coverage and improve the measurement of ITN use: Net distribution should continue, with particular attention to Sokoto and other areas of low or erratic coverage, and net-use data should be collected at a finer level so that its effect on malaria can be measured more reliably.
v. Strengthen surveillance and modelling capacity: Consistent testing and complete, timely reporting would help separate real changes in incidence from changes in detection, and training in spatial-temporal modelling would let ministries update risk maps and trends routinely.
vi. Future work should use finer spatial and temporal units, such as local government areas and monthly or seasonal data, to improve detection of nonlinear environmental effects and local transmission patterns.

Acknowledgements

The authors acknowledge the National Malaria Elimination Programme, Federal Ministry of Health, Nigeria, for the DHIS2 malaria case data; the National Population Commission, ICF (Demographic and Health Survey) and the National Bureau of Statistics for the poverty and ITN indicators; WorldPop, University of Southampton, for the population data; Google Earth Engine and the providers of the TerraClimate, ERA5-Land, MODIS, Landsat, SRTM and ESA WorldCover datasets for the environmental data; and the GADM database for the administrative boundaries.

Data Availability

The analysis used publicly available secondary data from DHIS2, Google Earth Engine datasets, WorldPop, the Nigeria Demographic and Health Survey, the National Bureau of Statistics and GADM.

REFERENCES

Abatzoglou, J. T., Dobrowski, S. Z., Parks, S. A., & Hegewisch, K. C. (2018). TerraClimate, a high-resolution global dataset of monthly climate and climatic water balance from 1958–2015. *Scientific Data, 5*, Article 170191. https://doi.org/10.1038/sdata.2017.191

Bakare, E. A., Olasupo, I. I., Imoudu, M., Abidemi, A., Daniel, D. O., Osikoya, S. A., Mogbojuri, O. A., Nwana, A. O., Oniyelu, D. O., Olorunfemi, R. D., Olagbami, O. S., Agboola, D. O., Ikediashi, S. I., Adedeji, A., Ikuseka, O., Fadairo, M., Odewale, O., Onwuka, I. G., Hansinon, A., … Ogban, G. I. (2026). Modelling the effect of long-lasting insecticidal nets on malaria transmission dynamics in Kebbi State, Nigeria. *Infectious Disease Modelling, 11*(3), 896–919. https://doi.org/10.1016/j.idm.2026.01.003

Bayode, T., & Siegmund, A. (2024). Identifying childhood malaria hotspots and risk factors in a Nigerian city using geostatistical modelling approach. *Scientific Reports, 14*, Article 5445. https://doi.org/10.1038/s41598-024-55003-x

Bhatt, S., Weiss, D. J., Cameron, E., Bisanzio, D., Mappin, B., Dalrymple, U., Battle, K. E., Moyes, C. L., Henry, A., Eckhoff, P. A., Wenger, E. A., Briët, O., Penny, M. A., Smith, T. A., Bennett, A., Yukich, J., Eisele, T. P., Griffin, J. T., Fergus, C. A., … Gething, P. W. (2015). The effect of malaria control on Plasmodium falciparum in Africa between 2000 and 2015. *Nature, 526*(7572), 207–211. https://doi.org/10.1038/nature15535

Bosson-Amedenu, S., Eyiah-Bediako, F., & Anafo, A. Y. (2026). Malaria incidence, severity and mortality in children under five in Ghana: Evidence from generalised additive models. *BMC Public Health, 26*, Article 653. https://doi.org/10.1186/s12889-025-25931-y

Cressie, N. A. C. (1993). *Statistics for spatial data (Rev. ed.)*. Wiley. https://doi.org/10.1002/9781119115151

Dambazau, Z. B., Cyril-Egware, K., Charles, O., Eshikhena, G., Adegbite, G., Akoma, D., Ojielo, N., Gayawan, E.,

Gadanya, M., Nelson, E., Sikiru, N. A., & Kaduru, C. (2025). Malaria transmission dynamics and the impact of treatment interventions in Kano State, Nigeria: A compartmental model approach. *PAMJ - One Health, 18*, Article 11. https://doi.org/10.11604/pamj-oh.2025.18.11.48342

Dawaki, S., Al-Mekhlafi, H. M., Ithoi, I., Ibrahim, J., Atroosh, W. M., Abdulsalam, A. M., Sady, H., Elyana, F. N., Adamu, A. U., Yelwa, S. I., Ahmed, A., Al-Areeqi, M. A., Subramaniam, L. R., Nasr, N. A., & Lau, Y.L. (2016). Is Nigeria winning the battle against malaria? Prevalence, risk factors and KAP assessment among Hausa communities in Kano State. *Malaria Journal, 15*, Article 351. https://doi.org/10.1186/s12936-016-1394-3

Didan, K. (2021). *MODIS/Terra vegetation indices 16-day L3 global 250m SIN grid V061* [Data set]. NASA EOSDIS Land Processes DAAC. https://doi.org/10.5067/MODIS/MOD13Q1.061

Eilers, P. H. C., & Marx, B. D. (1996). Flexible smoothing with B-splines and penalties. *Statistical Science, 11*(2), 89–121. https://doi.org/10.1214/ss/1038425655

Ekpa, D. E., Salubi, E. A., Olusola, J. A., & Akintade, D. (2023). Spatio-temporal analysis of environmental and climatic factors impacts on malaria morbidity in Ondo State, Nigeria. *Heliyon, 9*(3), Article e14005. https://doi.org/10.1016/j.heliyon.2023.e14005

Eshofonie, F., Johnson, O., & Gayawan, E. (2025). Co-morbidity of malaria and soil-transmitted helminths in Nigeria: A joint Bayesian modelling approach. *Infectious Diseases of Poverty, 14*, Article 28. https://doi.org/10.1186/s40249-025-01276-x

Farr, T. G., Rosen, P. A., Caro, E., Crippen, R., Duren, R., Hensley, S., Kobrick, M., Paller, M., Rodriguez, E., Roth, L., Seal, D., Shaffer, S., Shimada, J., Umland, J., Werner, M., Oskin, M., Burbank, D., & Alsdorf, D. (2007). The Shuttle Radar Topography Mission. *Reviews of Geophysics, 45*(2), Article RG2004. https://doi.org/10.1029/2005RG000183

Federal Ministry of Health and Social Welfare of Nigeria, National Population Commission, & ICF. (2025). *Nigeria demographic and health survey 2024*. https://www.health.gov.ng/wp-content/uploads/2025/10/NDHS-2024-Final-Report_Disseminated17102025.pdf

GADM. (2022). *GADM database of global administrative areas (Version 4.1)* [Data set]. https://gadm.org

Githeko, A. K., Lindsay, S. W., Confalonieri, U. E., & Patz, J. A. (2000). Climate change and vector-borne diseases: A regional analysis. *Bulletin of the World Health Organization, 78*(9), 1136–1147. https://iris.who.int/handle/10665/268220

Gorelick, N., Hancher, M., Dixon, M., Ilyushchenko, S., Thau, D., & Moore, R. (2017). Google Earth Engine: Planetary-scale geospatial analysis for everyone. *Remote Sensing of Environment, 202*, 18–27. https://doi.org/10.1016/j.rse.2017.06.031

Hastie, T. J., & Tibshirani, R. J. (1990). *Generalized additive models*. Chapman & Hall. https://www.routledge.com/p/book/9780412343902

Isiko, I., Nyegenye, S., Bett, D. K., Asingwire, J. M., Okoro, L. N., Emeribe, N. A., Koech, C. C., Ahgu, O., Bulus, N. G., Taremwa, K., & Mwesigwa, A. (2024). Factors associated with the risk of malaria among children: Analysis of 2021 Nigeria Malaria Indicator Survey. *Malaria Journal, 23*, Article 109. https://doi.org/10.1186/s12936-024-04939-6

Kammann, E. E., & Wand, M. P. (2003). Geoadditive models. *Journal of the Royal Statistical Society: Series C (Applied Statistics), 52*(1), 1–18. https://doi.org/10.1111/1467-9876.00385

McCullagh, P., & Nelder, J. A. (1989). *Generalized linear models (2nd ed.)*. Chapman & Hall. https://www.routledge.com/p/book/9780412317606

Mordecai, E. A., Paaijmans, K. P., Johnson, L. R., Balzer, C., Ben-Horin, T., de Moor, E., McNally, A., Pawar, S., Ryan, S. J., Smith, T. C., & Lafferty, K. D. (2013). Optimal temperature for malaria transmission is dramatically lower than previously predicted. *Ecology Letters, 16*(1), 22–30. https://doi.org/10.1111/ele.12015

Muñoz-Sabater, J., Dutra, E., Agustí-Panareda, A., Albergel, C., Arduini, G., Balsamo, G., Boussetta, S., Choulga, M., Harrigan, S., Hersbach, H., Martens, B., Miralles, D. G., Piles, M., Rodríguez-Fernández, N. J., Zsoter, E., Buontempo, C., & Thépaut, J.N. (2021). ERA5-Land: A state-of-the-art global reanalysis dataset for land applications. *Earth System Science Data, 13*(9), 4349–4383. https://doi.org/10.5194/essd-13-4349-2021

National Malaria Elimination Programme, National Population Commission, & ICF. (2022). *Nigeria malaria indicator survey 2021 final report*. https://dhsprogram.com/pubs/pdf/MIS41/MIS41.pdf

Nelder, J. A., & Wedderburn, R. W. M. (1972). Generalized linear models. *Journal of the Royal Statistical Society: Series A (General), 135*(3), 370–384. https://doi.org/10.2307/2344614

Odhiambo, J. N., Kalinda, C., Macharia, P. M., Snow, R. W., & Sartorius, B. (2020). Spatial and spatio-temporal methods for mapping malaria risk: A systematic review. *BMJ Global Health, 5*(10), Article e002919. https://doi.org/10.1136/bmjgh-2020-002919

Ogbuagada, S. O., Okolo, A., Torsen, E., & John, O. T. (2022). Multivariate time series analysis in modelling malaria cases in Jimeta metropolis of Adamawa State, Nigeria. *FUDMA Journal of Sciences, 6*(3), 62–69. https://doi.org/10.33003/fjs-2022-0603-970

Ogidan, O. C., Nzoputam, C. I., Barrow, A., & Ekholuenetale, M. (2025). Prevalence and determinants of insecticide-treated net ownership among women of reproductive age in Nigeria: A mixed-effect insight from the 2021 malaria indicator survey. *Malaria Journal, 24*, Article 75. https://doi.org/10.1186/s12936-025-05314-9

Ogunsakin, R. E., Babalola, B. T., Olusola, J. A., Joshua, A. O., & Okpeku, M. (2024). GIS-based spatiotemporal mapping of malaria prevalence and exploration of environmental inequalities. *Parasitology Research, 123*, Article 262. https://doi.org/10.1007/s00436-024-08276-0

Patz, J. A., Campbell-Lendrum, D., Holloway, T., & Foley, J. A. (2005). Impact of regional climate change on human health. *Nature, 438*(7066), 310–317. https://doi.org/10.1038/nature04188

R Core Team. (2024). *R: A language and environment for statistical computing*. R Foundation for Statistical Computing. https://www.R-project.org/

Roy, D. P., Wulder, M. A., Loveland, T. R., Woodcock, C. E., Allen, R. G., Anderson, M. C., Helder, D., Irons, J. R., Johnson, D. M., Kennedy, R., Scambos, T. A., Schaaf, C. B., Schott, J. R., Sheng, Y., Vermote, E. F., Belward, A. S., Bindschadler, R., Cohen, W. B., Gao, F., Zhu, Z. (2014). Landsat-8: Science and product vision for terrestrial global change research. *Remote Sensing of Environment, 145*, 154–172. https://doi.org/10.1016/j.rse.2014.02.001

Tatem, A. J., Gething, P. W., Smith, D. L., & Hay, S. I. (2013). Urbanization and the global malaria recession. *Malaria Journal, 12*, Article 133. https://doi.org/10.1186/1475-2875-12-133

Tibshirani, R. (1996). Regression shrinkage and selection via the lasso. *Journal of the Royal Statistical Society: Series B (Methodological), 58*(1), 267–288. https://doi.org/10.1111/j.2517-6161.1996.tb02080.x

Tobler, W. R. (1970). A computer movie simulating urban growth in the Detroit region. *Economic Geography, 46*(Suppl. 1), 234–240. https://doi.org/10.2307/143141

Ugwu, C. L. J., & Zewotir, T. (2020). Evaluating the effects of climate and environmental factors on under-5 children malaria spatial distribution using generalized additive models (GAMs). *Journal of Epidemiology and Global Health, 10*(4), 304–314. https://doi.org/10.2991/jegh.k.200814.001

Wood, S. N. (2011). Fast stable restricted maximum likelihood and marginal likelihood estimation of semiparametric generalized linear models. *Journal of the Royal Statistical Society: Series B (Statistical Methodology), 73*(1), 3–36. https://doi.org/10.1111/j.1467-9868.2010.00749.x

Wood, S. N. (2017). *Generalized additive models: An introduction with R (2nd ed.)*. Chapman & Hall/CRC. https://doi.org/10.1201/9781315370279

World Health Organization. (2024). *World malaria report 2024: Addressing inequity in the global malaria response*. https://www.who.int/teams/global-malaria-programme/reports/world-malaria-report-2024

WorldPop. (n.d.). *Open spatial demographic data and research*. University of Southampton. Retrieved October 25, 2026, from https://www.worldpop.org/

Yakudima, I. I., Adamu, Y. M., Samat, N., Mohammed, M. U., Abdulkarim, I. I., & Hassan, N. I. (2024). Geospatial analysis of malaria prevalence among children under five years in Jigawa State, North West, Nigeria. *African Journal of Biomedical Research, 27*(2), 243–251. https://www.ajol.info/index.php/ajbr/article/view/278784

Yamana, T. K., & Eltahir, E. A. B. (2013). Incorporating the effects of humidity in a mechanistic model of Anopheles gambiae mosquito population dynamics in the Sahel region of Africa. *Parasites & Vectors, 6*, Article 235. https://doi.org/10.1186/1756-3305-6-235

Zanaga, D., Van De Kerchove, R., De Keersmaecker, W., Souverijns, N., Brockmann, C., Quast, R., Wevers, J., Grosu, A., Paccini, A., Vergnaud, S., Cartus, O., Santoro, M., Fritz, S., Georgieva, I., Lesiv, M., Carter, S., Herold, M., Li, L., Tsendbazar, N.-E., … Arino, O. (2021). *ESA WorldCover 10 m 2020 v100* [Data set]. Zenodo. https://doi.org/10.5281/zenodo.5571936

Zhang, S., Amratia, P., Symons, T. L., Rumisha, S. F., Kang, S. Y., Connell, M., Uusiku, P., Katokele, S., Hamunyela, J., Ntusi, N., Soroses, W., Moyo, E., Lukubwe, O., Maponga, C., Lucero, D., Gething, P. W., & Cameron, E. (2024). High-resolution spatio-temporal risk mapping for malaria in Namibia: A comprehensive analysis. *Malaria Journal, 23*, Article 297. https://doi.org/10.1186/s12936-024-05103-w

Zou, H., & Hastie, T. (2005). Regularization and variable selection via the elastic net. *Journal of the Royal Statistical Society: Series B (Statistical Methodology), 67*(2), 301–320. https://doi.org/10.1111/j.1467-9868.2005.00503.x

©2026 This is an Open Access article distributed under the terms of the Creative Commons Attribution 4.0 International license viewed via https://creativecommons.org/licenses/by/4.0/ which permits unrestricted use, distribution, and reproduction in any medium, provided the original work is cited appropriately.